AIMETA 2017
XXIII Conference
The Italian Association of Theoretical and Applied Mechanics
Luigi Ascione, Valentino Berardi, Luciano Feo, Fernando Fraternali and Antonio Michele Tralli (eds.)
Salerno, Italy, 4-7 September 2017

EXPERIMENTAL VALIDATION OF THE ENHANCED BEAM-THEORY MODEL OF THE MIXED-MODE BENDING TEST

Stefano Bennati[1], **Paolo Fisicaro**[1], **Luca Taglialegne**[1], **and Paolo S. Valvo**[1]

[1] Department of Civil and Industrial Engineering, University of Pisa
Largo Lucio Lazzarino, 56122 Pisa (PI)
e-mail: {s.bennati, p.fisicaro, l.taglialegne, p.valvo}@ing.unipi.it

Keywords: Composite laminate, delamination, mixed-mode bending test.

Abstract. *We present the results of an experimental campaign on a set of specimens manufactured from a typical carbon/epoxy unidirectional laminate. Preliminary tests are performed to evaluate the elastic properties of the base laminate. Then, double cantilever beam (DCB) and end-notched flexure (ENF) tests are conducted to assess the delamination toughness in pure fracture modes I and II, respectively, and evaluate the elastic interface constants. Afterwards, mixed-mode bending (MMB) tests are carried out with three values of the lever-arm length. The outcomes of the preliminary and pure fracture mode tests are used as an input to a previously developed enhanced beam theory (EBT) model of the MMB test. Lastly, theoretical predictions and experimental results are compared.*

1 INTRODUCTION

Composite materials are subject to a variety of damage phenomena at both the microscopic and macroscopic scales. Analysis of delamination failure is usually conducted through energetic principles derived in the context of Fracture Mechanics [1]. Several testing procedures are used to measure delamination toughness of composite laminates [2]. For pure fracture modes I and II, the *double cantilever beam* (DCB) [3] and *end-notched flexure* (ENF) [4] tests are used, respectively. For I/II mixed-mode fracture, the *mixed-mode bending* (MMB) test has been standardised by ASTM for unidirectional laminates. Assuming linear behaviour, the MMB test can be considered as the superposition of the DCB and ENF tests [5].

We have developed an enhanced beam theory (EBT) model of the MMB test, whereby the specimen is considered as an assemblage of two identical sublaminates, modelled as laminated Timoshenko beams. The sublaminates are partly connected by a linearly elastic–brittle interface, transmitting both normal and shear stresses. In previous works, an explicit solution of this problem – with analytical expressions for the specimen compliance, energy release rate, and mode mixity – has been obtained. This solution yields, as special cases, the solutions for the DCB and ENF tests [6, 7]. Based on the latter, an experimental compliance calibration strategy has been proposed to evaluate the constants of the elastic interface [8]. Recently, the model has been applied to predict also the response of the MMB test under cyclic loads by introducing a fracture mode-dependent fatigue growth law [9].

Here, we present the results of an experimental campaign on a set of carbon/epoxy unidirectional laminated specimens. Preliminary tests are performed to evaluate the elastic properties of the base laminate. Then, DCB and ENF tests are conducted to assess the delamination toughness in pure fracture modes I and II, respectively, and evaluate the elastic interface constants. Afterwards, MMB tests are carried out with three values of the lever-arm length. The outcomes of the preliminary and pure fracture mode tests are used as an input to the EBT model of the MMB test. Lastly, theoretical predictions and experimental results are compared.

2 ENHANCED BEAM THEORY MODEL OF THE MMB TEST

2.1 Mechanical model

In the MMB test, a laminated specimen with a delamination of length a is simply supported and loaded through a rigid lever (Fig. 1a). We denote with $L = 2\ell$, B, and H the length, width, and thickness of the specimen, respectively. The delamination divides the specimen into two sublaminates, each of thickness $h = H/2$. The load applied by the testing machine, P, is transferred to the specimen as a combination of an upward load, P_u, and a downward load, P_d, respectively applied at the delaminated end and mid-span cross sections. The lever-arm length, c, can be adjusted to vary the intensities of P_u and P_d, thus imposing a desired ratio, $G_\mathrm{I}/G_\mathrm{II}$, of the energy release rates associated to fracture modes I and II. Global reference x- and z-axes are aligned with the specimen longitudinal and transverse directions, respectively.

In the enhanced beam theory model [6, 7], the specimen is regarded as an assemblage of sublaminates. Accordingly, let A_1, C_1, and D_1 be the sublaminate extensional, shear, and bending stiffnesses, respectively [10]. For unidirectional laminated specimens, $A_1 = E_x h$, $C_1 = 5\,G_{zx}h/6$, and $D_1 = E_x h^3/12$, where E_x and G_{zx} are the longitudinal Young's modulus and transverse shear modulus, respectively. The sublaminates are partly connected by an elastic–brittle interface. Let k_z and k_x be the elastic constants of the distributed springs, respectively acting along the normal and tangential directions with respect to the interface plane (Fig. 1b). The mathematical formulation of the problem and its detailed solution are available in the cited references [6, 7]. Here, only the final useful expressions are recalled.

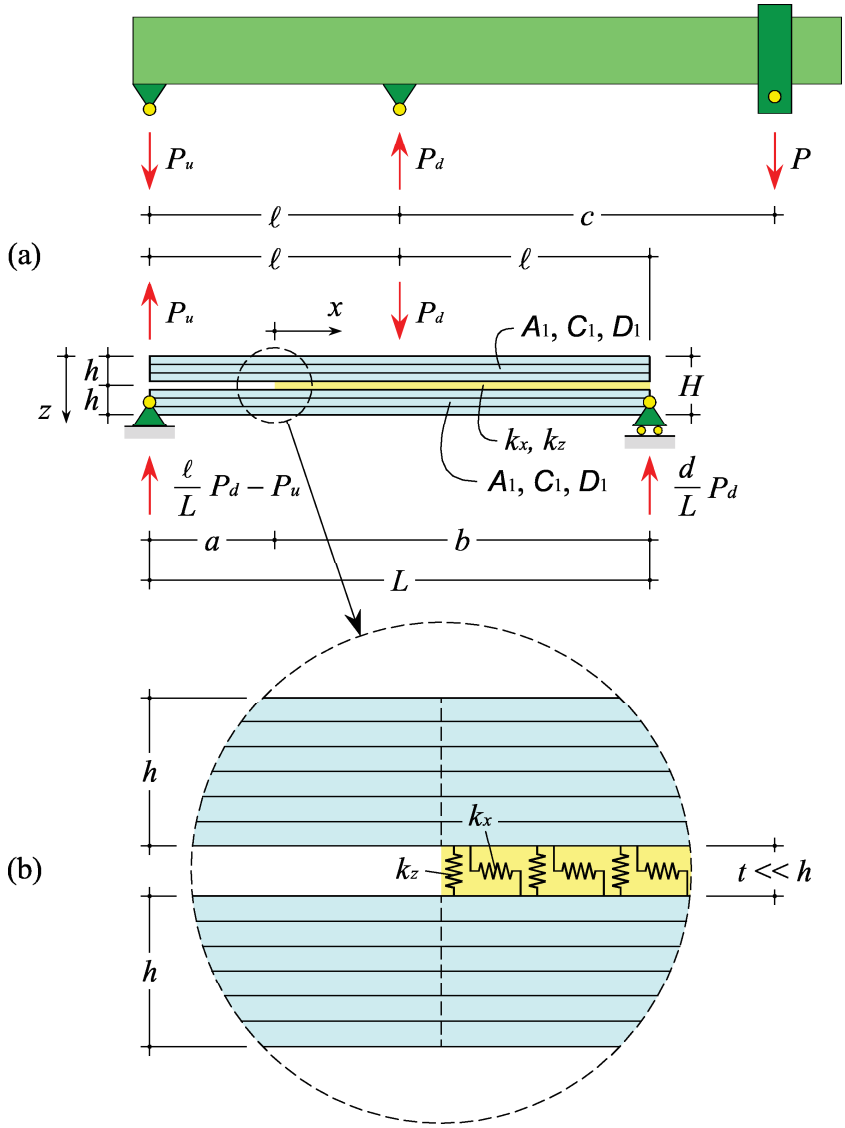

Figure 1: (a) MMB test specimen with loading lever and (b) detail of the crack-tip region and elastic interface.

2.2 Compliance

For linearly elastic load-deflection response, the compliance of a test specimen is defined as $C = \delta/P$, where P is the applied load and δ is the displacement of the load application point [2]. The compliance of the MMB test specimen turns out to be

$$C_{\mathrm{MMB}} = \left(\frac{3c-\ell}{4\ell}\right)^2 C_{\mathrm{DCB}} + \left(\frac{c+\ell}{\ell}\right)^2 C_{\mathrm{ENF}}, \tag{1}$$

where, according to our model,

$$C_{\mathrm{DCB}} = \frac{2a^3}{3BD_1} + \frac{2a}{BC_1} + \frac{2}{\lambda_1\lambda_2 BD_1}\left[\left(\lambda_1+\lambda_2\right)a^2 + 2a + \frac{1}{\lambda_1} + \frac{1}{\lambda_2}\right] \tag{2}$$

and

$$C_{\mathrm{ENF}} = \frac{1}{24B}\frac{A_1 h^2}{A_1 h^2 + 4D_1}\left(\frac{a^3}{D_1} + \frac{8\ell^3}{A_1 h^2}\right) + \frac{\ell}{4BC_1} + \\ + \frac{1}{8BD_1}\frac{A_1 h^2}{A_1 h^2 + 4D_1}\frac{1}{\lambda_5^2}\left[\lambda_5 a^2 + a + 2\ell - \frac{2}{\lambda_5} - \frac{4a}{\exp\lambda_5(\ell - a)}\right] \tag{3}$$

are the compliances of the DCB and ENF test specimens, respectively [7]. Furthermore,

$$\lambda_1 = \sqrt{\frac{k_z}{C_1}\left(1 + \sqrt{1 - \frac{2C_1^2}{k_z D_1}}\right)}, \quad \lambda_2 = \sqrt{\frac{k_z}{C_1}\left(1 - \sqrt{1 - \frac{2C_1^2}{k_z D_1}}\right)}, \text{ and } \lambda_5 = \sqrt{2k_x\left(\frac{1}{A_1} + \frac{h^2}{4D_1}\right)} \tag{4}$$

are the roots of the characteristic equations of the governing differential problem [6].

Eqs. (2) and (3) show that both C_{DCB} and C_{ENF} are the sums of three contributions, respectively depending on the sublaminate bending stiffness (Euler-Bernoulli beam theory), the transverse shear deformability (Timoshenko's beam theory), and the elastic interface. Both C_{DCB} and C_{ENF} are expressed by cubic polynomials of the delamination length, a, except for an exponential term (negligible in most cases) appearing in the expressions for C_{ENF}. Thus, the EBT model provides a rationale for some semi-empirical relationships of the literature [11]. Furthermore, since C_{DCB} depends on k_z (through λ_1 and λ_2) and C_{ENF} depends on k_x (through λ_5), Eqs. (2) and (3) offer a basis to evaluate the elastic interface constants from experimental results of DCB and ENF tests [8].

2.3 Energy release rate

Under I/II mixed-mode fracture conditions, the energy release rate can be written as $G = G_{\mathrm{I}} + G_{\mathrm{II}}$, where G_{I} and G_{II} are the contributions related to fracture modes I and II, respectively. For the MMB test specimen,

$$G_{\mathrm{I}} = \frac{P_{\mathrm{I}}^2}{2B}\frac{dC_{\mathrm{DCB}}}{da} \text{ and } G_{\mathrm{II}} = \frac{P_{\mathrm{II}}^2}{2B}\frac{dC_{\mathrm{ENF}}}{da}, \tag{5}$$

where

$$P_{\mathrm{I}} = \frac{3c - \ell}{4\ell}P \text{ and } P_{\mathrm{II}} = \frac{c + \ell}{\ell}P \tag{6}$$

are the loads responsible for fracture modes I and II, respectively. By substituting Eqs. (2) and (3) into (5), we obtain

$$G_{\mathrm{I}} = \frac{P_{\mathrm{I}}^2}{B^2 D_1}\left(a + \chi_{\mathrm{I}} h\right)^2 \text{ and } G_{\mathrm{II}} \cong \frac{P_{\mathrm{II}}^2}{16B^2 D_1}\frac{A_1 h^2}{A_1 h^2 + 4D_1}\left(a + \chi_{\mathrm{II}} h\right)^2, \tag{7}$$

where

$$\chi_{\mathrm{I}} = \frac{1}{h}\left(\frac{1}{\lambda_1} + \frac{1}{\lambda_2}\right) = \frac{1}{h}\sqrt{\frac{D_1}{C_1} + \sqrt{\frac{2D_1}{k_z}}} \text{ and } \chi_{\mathrm{II}} = \frac{1}{h}\frac{1}{\lambda_5} = \frac{1}{h}\Bigg/\sqrt{2k_x\left(\frac{1}{A_1} + \frac{h^2}{4D_1}\right)} \tag{8}$$

are crack length correction parameters [7]. Eqs. (8) can be regarded as a generalisation for multidirectional laminates of the formulas given by the ASTM standard [5] for unidirectional laminated specimens.

2.4 Mode mixity

To characterise the relative contributions of fracture modes I and II, we introduce the mode-mixity angle,

$$\psi = \arctan\sqrt{\frac{G_{\mathrm{II}}}{G_{\mathrm{I}}}}\,. \tag{9}$$

For the MMB test specimen, by substituting Eqs. (6) and (7) into (9), we obtain

$$\psi = \arctan\frac{1}{\beta\dfrac{3c-\ell}{c+\ell}\sqrt{1+4D_1/\left(A_1h^2\right)}}\,, \tag{10}$$

where

$$\beta = \frac{a+\chi_{\mathrm{I}}h}{a+\chi_{\mathrm{II}}h} = \frac{a+1/\lambda_1+1/\lambda_2}{a+1/\lambda_5}. \tag{11}$$

Eq. (10) can be solved to obtain the lever-arm length yielding a desired mode mixity,

$$c = \frac{\beta\sqrt{1+4D_1/\left(A_1h^2\right)}\tan\psi+1}{3\beta\sqrt{1+4D_1/\left(A_1h^2\right)}\tan\psi-1}\,\ell\,. \tag{12}$$

3 EXPERIMENTAL TESTS

To validate the developed theoretical model, we have conducted an experimental campaign on unidirectional laminated specimens obtained from a typical carbon fibre/epoxy matrix composite laminate. First, the elastic properties of the base laminate have been determined through three-point bending tests on specimens with no delamination. By following a procedure similar to that proposed in [12], the following average values have been obtained: longitudinal Young's modulus E_x = 117.7 GPa, transverse shear modulus G_{zx} = 1.42 GPa. Then, various delamination toughness tests have been conducted on a set of 7 delaminated specimens. The overall length of each specimen was 250 mm. This has allowed each specimen to be tested under several testing configurations, *e.g.* first a DCB test, until the delamination had propagated to a certain length, and then another configuration, *e.g.* ENF or MMB tests. This is in line with standard testing procedures in fracture modes I and II [3, 4]. Table 1 shows the cross-section sizes and the performed tests of each specimen.

Specimen #	Width B (mm)	Height H (mm)	Tests
1	25.15	3.23	MMB, ENF
2	25.18	3.24	MMB, ENF
3	25.18	3.24	DCB, MMB
4	25.14	3.20	DCB, MMB
5	25.04	3.13	DCB, MMB
6	25.27	3.19	DCB, MMB, ENF
7	25.20	3.09	DCB, MMB, ENF
Average	25.16	3.18	–

Table 1: Geometry of tested specimens.

Figures 2a and 2b show typical load, P, vs. displacement, δ, curves obtained from the DCB and ENF tests, respectively. In order to apply the experimental compliance calibration strategy to evaluate the elastic interface constants, k_x and k_z, it is necessary to measure the values of the specimen compliances, C_{DCB} and C_{ENF}, at different values of delamination length, a [8]. In DCB tests, crack propagation is stable, so that this objective can be achieved simply by correlating the measured values of P and δ during the crack propagation stage with the corresponding values of a. In ENF tests, since crack propagation is generally unstable (for $a < 0.7\,\ell$) [13], a different strategy has to be used. In this study, we have conducted the ENF tests by first loading and unloading the specimens within the elastic range of behaviour, *i.e.* without achieving crack propagation, at several values of the delamination length. The main outcomes of the DCB and ENF tests are summarised in Table 2.

For comparison, the theoretical predictions of the EBT model for the performed tests are shown with dashed black lines on the same plots in figure 2. The curves in the linearly elastic range of behaviour are obtained from the model by assuming the average values of k_x and k_z. The curves in the crack propagation stage correspond to the fulfilment of the pure mode I and mode II propagation criteria, $G = G_I = G_{Ic}$ and $G = G_{II} = G_{IIc}$, respectively, with the average delamination toughness values obtained from the tests (Table 2).

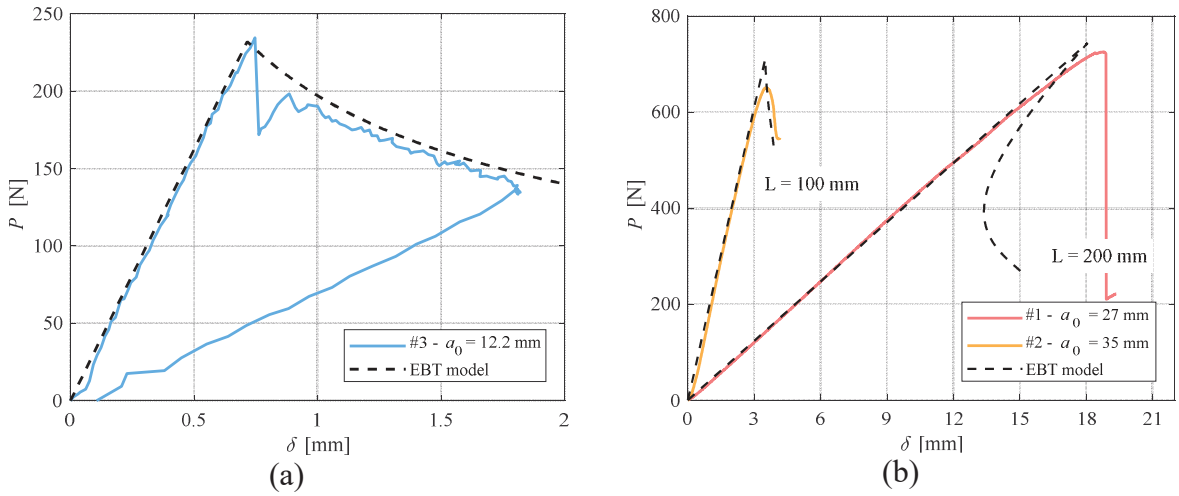

Figure 2: Typical load-displacement curves from (a) DCB and (b) ENF tests.

	DCB tests		ENF tests	
Specimen #	Normal spring constant k_z (N/mm^3)	Mode I delamination toughness G_{Ic} (N/m)	Tangential spring constant k_x (N/mm^3)	Mode II delamination toughness G_{IIc} (N/m)
1	–	–	3.297×10^3	1516.3
2	–	–	3.287×10^3	1567.2
3	3.046×10^4	604.6	–	–
4	9.919×10^2	447.0	–	–
5	4.885×10^3	560.2	–	–
6	5.632×10^3	655.8	3.340×10^3	1604.1
7	2.455×10^5	693.6	3.441×10^3	1170.8
Average	5.750×10^4	592.2	3.340×10^3	1464.6

Table 2: Results of DCB and ENF tests.

Figure 3 shows the load vs. displacement curves obtained from the MMB tests. For comparison, the theoretical predictions of the EBT model are shown with dashed black lines on the same plots. The curves in the linearly elastic range of behaviour are obtained from the model by assuming average values of k_x and k_z. The curves in the crack propagation stage are obtained by assuming the following elliptical mixed-mode crack-growth criterion [9]:

$$\left(\frac{G_{\mathrm{I}}}{G_{\mathrm{Ic}}}\right)^2+\left(\frac{G_{\mathrm{II}}}{G_{\mathrm{IIc}}}\right)^2=1. \tag{13}$$

The latter can be shown to be equivalent to consider $G = G_c$ with the following definition of fracture mode-dependent delamination toughness:

$$G_{\mathrm{c}}(\psi)=\frac{1}{\sqrt{\dfrac{\cos^4\psi}{G_{\mathrm{Ic}}^2}+\dfrac{\sin^4\psi}{G_{\mathrm{IIc}}^2}}}. \tag{14}$$

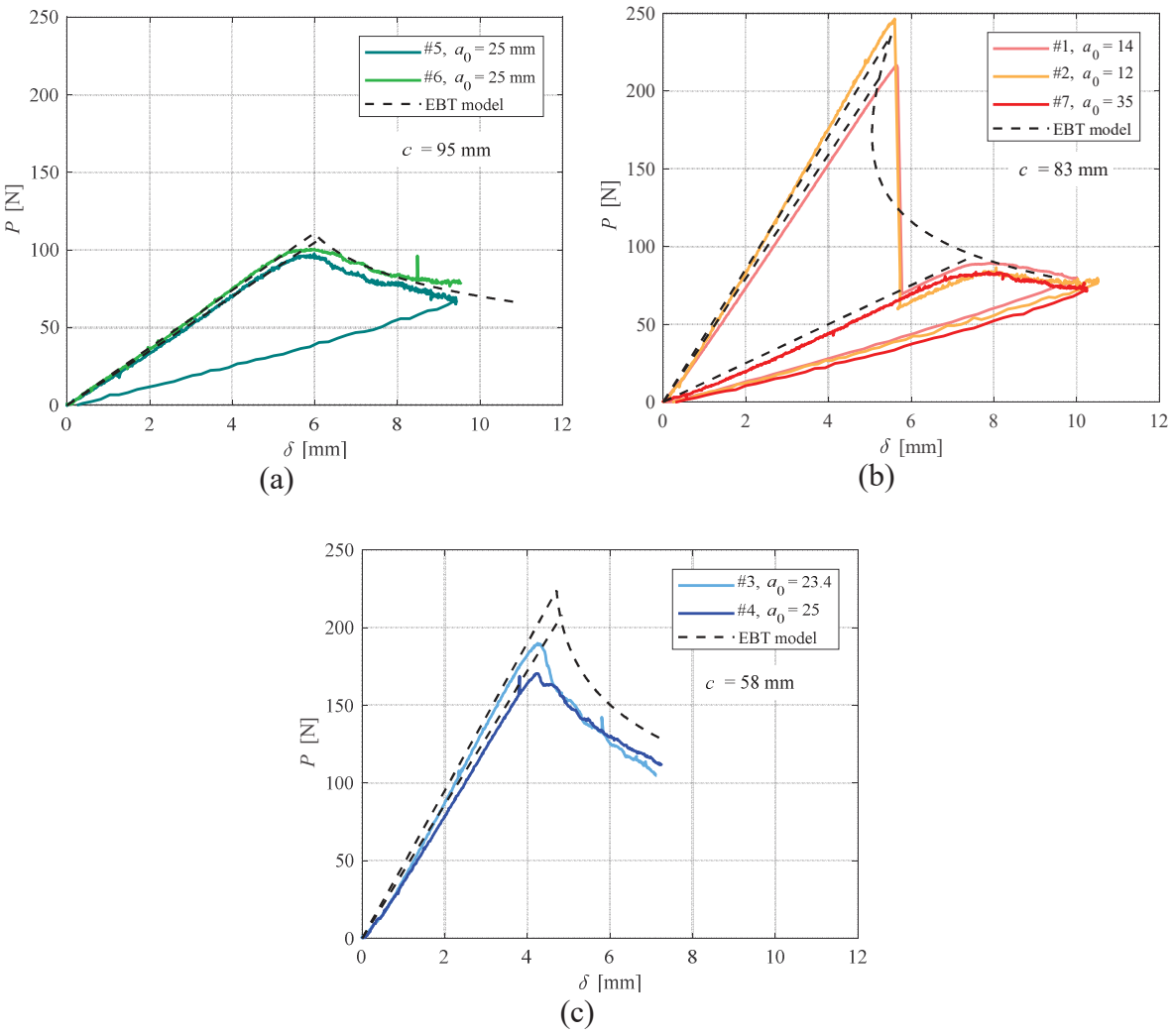

Figure 3: Load-displacement curves from MMB tests with lever-arm length (a) c = 95 mm, (b) c = 83 mm, and (c) c = 58 mm.

Figure 4a shows the values of G_{I} vs. G_{II} at the onset of delamination growth in the MMB tests, as computed through Eqs. (7) with (6) and (8). The dashed black line represents the corresponding values as computed through the mixed-mode crack-growth criterion Eq. (13). Figure 4b shows the total G at the onset of delamination growth as a function of the mode-mixity angle, ψ, as computed from Eq. (9). For comparison, the dashed black line represents the critical energy release rate as given by Eq. (14).

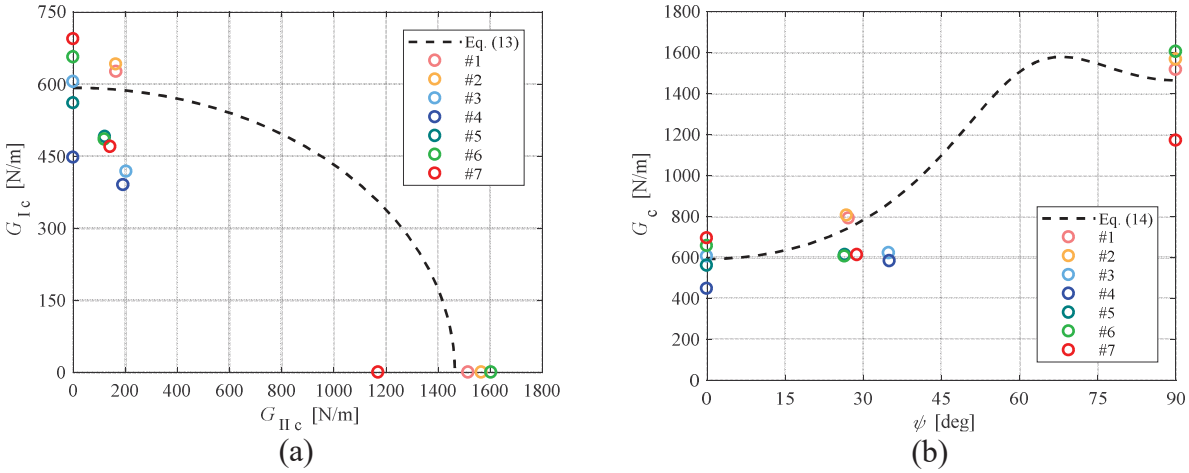

Figure 4: Critical energy release rate at the onset of delamination growth in MMB tests: (a) mode I vs. mode II contributions; (b) total energy release rate vs. mode-mixity angle.

4 CONCLUSIONS

We have presented the results of an experimental campaign aiming at validating a previously developed analytical solution for an enhanced beam theory model of the MMB test specimen. Preliminary tests have been performed to evaluate the elastic properties of the base material consisting of a typical carbon/epoxy unidirectional laminate. Then, DCB and ENF test have been conducted to assess the delamination toughness in pure fracture modes I and II, respectively. Besides, an experimental compliance calibration procedure has been applied to evaluate the elastic interface constants. Lastly, MMB tests have been conducted with three values of the lever-arm length. Based on the preliminary and pure fracture mode test results, predictions have been made for the MMB tests by using the enhanced beam theory model. A good agreement between the theoretical predictions and experimental results has been obtained.

5 ACKNOWLEDGEMENTS

The authors wish to thank (not in order of relevance):

- the CETMA consortium, Brindisi, for the careful manufacture of the test specimens;
- Prof. Luigi Lazzeri and the Laboratory technicians of the Division of Aerospace Engineering of the Department of Civil and Industrial Engineering of the University of Pisa for the execution of the DCB and MMB tests;
- Prof. Marco Paggi and Dr. Claudia Borri of IMT School for Advanced Studies, Lucca, for the executions of the three-point bending and ENF tests.

REFERENCES

[1] R. Talreja, C.V. Singh, *Damage and Failure of Composite Materials*. Cambridge University Press, 2012.

[2] L.A. Carlsson, D.F. Adams, R.B. Pipes, *Experimental Characterization of Advanced Composite Materials, 4th Edition*. CRC Press, 2014.

[3] *prEN 6033 P1, Carbon fibre reinforced plastics – Test method – Determination of interlaminar fracture toughness energy – Mode I Gic*. ASD-STAN, 1995.

[4] *prEN 6034 P1, Carbon fibre reinforced plastics – Test method – Determination of interlaminar fracture toughness energy – Mode II Giic*. ASD-STAN, 1995.

[5] *ASTM D6671/D6671M-13e1, Standard Test Method for Mixed Mode I-Mode II Interlaminar Fracture Toughness of Unidirectional Fiber Reinforced Polymer Matrix Composites*. ASTM International, 2013.

[6] S. Bennati, P. Fisicaro, P.S. Valvo, An enhanced beam-theory model of the mixed-mode bending (MMB) test – Part I: literature review and mechanical model. *Meccanica*, **48**, 443-462, 2013.

[7] S. Bennati, P. Fisicaro, P.S. Valvo, An enhanced beam-theory model of the mixed-mode bending (MMB) test – Part II: applications and results. *Meccanica*, **48**, 465-484, 2013.

[8] S. Bennati, P.S. Valvo, An experimental compliance calibration strategy for mixed-mode bending tests. *Procedia Materials Science*, **3**, 1988-1993, 2014.

[9] S. Bennati, P. Fisicaro, P.S. Valvo, An elastic-interface model for the mixed-mode bending test under cyclic loads, *Procedia Structural Integrity*, **2**, 72-79, 2016.

[10] R.M. Jones, *Mechanics of composite materials, 2nd Edition*. Taylor & Francis, 1999.

[11] R.H. Martin, P.L. Hansen, Experimental compliance calibration for the mixed-mode bending (MMB) specimen. In: E.A. Armanios (Ed.), *Composite Materials: Fatigue and Fracture, Sixth Volume*. ASTM STP 1285, 305-323, 1997.

[12] F. Mujika, On the effect of shear on local deformation in three-point bending test. *Polymer Testing*, **26**, 869-877, 2007.

[13] L.A. Carlsson, J.W. Gillespie Jr, R.B. Pipes, On the Analysis and Design of the End Notched Flexure (ENF) Specimen for Mode II Testing. *Journal of Composite Materials*, **20**, 594-604, 1986.